Impact of Lithium pellets on the plasma performance in the all-metal-wall tokamak ASDEX Upgrade

P. T. Lang[1], R. Maingi[2], D.K. Mansfield[2], R. McDermott[1], R. Neu[1,3], E. Wolfrum[1], R. Arredondo Parra[1], M. Bernert[1], G. Birkenmeier[1,3], A. Diallo[2], M. Dunne[1], E. Fable[1], R. Fischer[1], B. Geiger[1], A. Hakola[4], G. Kocsis[5], F. Laggner[1], M. Oberkofler[1], B. Ploeckl[1], B. Sieglin[1], ASDEX Upgrade Team

1) MPI für Plasmaphysik, Boltzmannstr. 2, 85748 Garching, Germany
2) Princeton Plasma Physics Laboratory, PO Box 451, Princeton, NJ 08543, USA
3) Technische Universität München, Boltzmannstr. 15, 85748 Garching, Germany
4) VTT Technical Research Centre of Finland Ltd., PO Box 1000, FI-02044 VTT, Finland
5) Wigner RCP RMI, Konkoly Thege u. 29 - 33, H - 1121 Budapest, Hungary

INTRODUCTION

Several tokamaks like NSTX [1], EAST [2] and DIII-D [3] have reported significant improvement in several key plasma parameters like pedestal pressure and width concurrent with the presence of lithium (Li) in the plasma. In addition rapid controlled triggering of small edge-localized modes (ELMs) thus creating more manageable transient heat loads was demonstrated by injecting small spherical lithium granules [4]. Li could thus offer pronounced advantages for future high power fusion devices, such as ITER and DEMO, by improving plasma performance and/or mitigating the ELMs. However, confinement improvement can equally well be attributed to wall conditioning effects or transients while the claim for reliable ELM control needs to be further investigated under various plasma scenarios. Hence, at ASDEX Upgrade (AUG) explorative experiments have been performed to find out if such effects can be observed also under reactor relevant conditions when operating with an all-metal-wall. In particular, our experiments aimed at Li deposition deep inside the plasma to keep the amount of Li low and minimize the impact on the first wall.

SET UP: ASDEX UPGRADE, LI PELLET LAUNCHER AND DIAGNOSTICS

AUG [5] is a mid-size divertor tokamak (major radius R_0 = 1.65 m, minor radius a_0 = 0.5 m) with all its plasma facing components completely covered with tungsten (W). The versatile set of auxiliary heating systems comprises 20 MW neutral beam injection (NI), up to 6 MW ion cyclotron resonance heating (ICRH), and 5 MW electron cyclotron resonance heating (ECRH). Investigations reported here were performed operating with the bulk tungsten divertor III configuration [6]. An interlock system monitoring several key plasma parameters is employed for machine protection; here it was employed to prevent pellet injection under unfavourable plasma conditions or after a disruption.

In order to focus on the impact Li has in the confined plasma, Li pellets providing a penetration deep into the plasma were used. To achieve this, a gas gun launcher was developed, with details presented elsewhere [7]. The launcher is capable of injecting pellets containing about 1.6 x 10^{20} Li atoms ($m_P \approx 1.9$ mg) at a rate up to 2 Hz. Its revolver plate magazine hosts 36 pellets stored in equally spaced holes of diameter 1.5 mm, preloaded by mechanical double-stage extrusion of the soft Li originating from a 6 mm diameter wire. During the entire Li pellet campaign about 100 attempts to launch pellets were made with about 80 of them successful (the rest were found still sticking in the magazine). This is in total only about 150 mg of Li launched into the vessel. Significant disturbance of the plasma by the propellant gas was avoided by selecting deuterium (D) as the propellant and minimizing the parasitic gas flux to the torus by installing an expansion tank and a strong cryo pump into the system. Useful propellant gas pressures range from 30 to 100 bar, resulting in pellet speeds of 420 - 700 m/s. For increasing the propellant gas pressure a reduced scattering angle of pellet

trajectories with respect to the designed path is observed. Thus, high reliability for pellet delivery can be achieved despite the narrow access cone to the plasma. However, a higher gas pressure causes more parasitic flux. The best compromise was achieved for a pressure of 50 bar, granting sufficient pellet delivery reliability while the resulting maximum parasitic flux to the torus vessel remained at about 6 x 10^{20} D/s, a value still significantly below typical applied gas puffing rates around 10^{22} D/s. For the according pellet speed of 600 m/s (typical speeds scatter about 20 m/s) sufficiently deep penetration was achieved.

AUG is equipped with a very versatile set of diagnostics capable of investigating the impact of Li in the core plasma. For monitoring the Li pellet ablation radiation, two extra diodes were installed collecting all visible light emitted in the designated ablation region, one observing from the top and one horizontally from behind the pellet gun. While the top view has a dynamical recording range adapted to the peak radiation and is hence capable of recording the entire ablation process with moderate sensitivity, the horizontal view has a very high sensitivity allowing for a precise determination of the pellet's separatrix crossing but at the expense of saturation during the peak ablation. The charge exchange recombination spectroscopy (CXRS) diagnostics was employed to obtain radial Li density profiles.

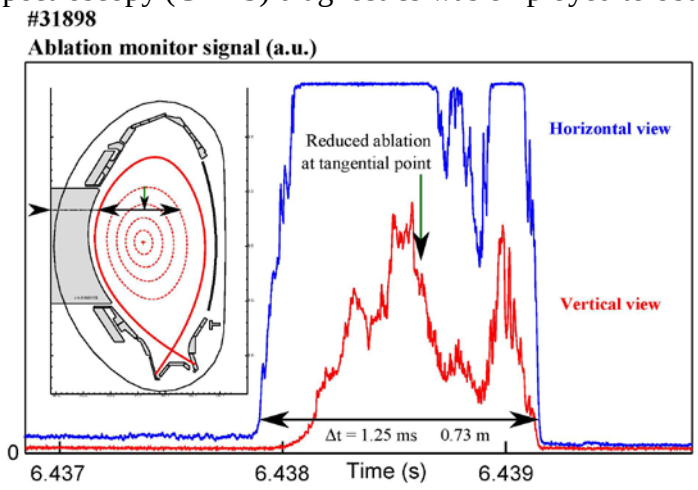

Figure 1: Temporal evolution of Li pellet ablation radiation recorded for the sensitive horizontally viewing diode and the survey vertical view. Assuming pellet flight along the designated path with a speed of 600 m/s the deposition range can be determined (insert). Once the pellet trajectory becomes tangential with respect to the flux surfaces, strong temporal local cooling of the plasma causes a sharp drop in radiation and presumably ablation rate.

EFFICIENT LI DEPOSITION IN THE CORE PLASMA

Beyond the ablation and initial deposition profile, presence, concentration and confinement time of the Li ions in the core and edge plasma were determined by several diagnostics. For example spectroscopy confirms the presence of Li in the entire plasma column after each successful injection of a pellet. Strong emission from hot ions is observed from the temperature broadened wing of the line at 516.8 nm attributed to the transition n = 7 → n = 5 of Li^{++} generated by charge exchange between fully stripped Li and D atoms injected by the NBI. However, the Li presence is lasting less than 500 ms and thus due to the maximum repetition rate of 2 Hz there is no pile up of Li in the plasma achieved. Hence, every single pellet can be considered as an individual event and analysed accordingly.

During its peak phase, the Li concentration (n_{Li}/n_e) in the plasma reaches approximately 0.15; the temporal evolution of the Li in the plasma after pellet injection is displayed in the lower part of figure 2. The electron density profile calculated from the Li profiles (blue dots in the upper part of figure 2) fits rather well to the observed impact on the n_e profile (solid blue line). For the Li profile obtained 12 ms after the pellet arrival, the effect of initial pellet penetration and deposition remains visible. However already at about 30 ms a nearly homogeneous doping across the entire plasma column is achieved with the Li profile becoming similar to the electron density n_e profile shown in the upper part of figure 2. The homogeneous high Li concentration is decaying for the case shown in figure 2 with a time constant of approximately 100 ms, and almost identical sustainment times are obtained when analysing e.g. the decay of the entire n_e inventory surplus or the Li radiation from different

radial positions. The observed evolution of the Li distribution during the decay phase was found in very good agreement with dedicated modelling results of the confinement region in a typical H-mode plasma using a combination of ASTRA and TGLF as the impurity turbulence-driven transport model [8]. Quite a range of different plasma scenarios has been used for Li pellet injection. At the restart for the AUG campaign 2015/2016, a variety of different commissioning discharges were performed, some especially tailored for implementing and characterisation of the Li launcher. Furthermore, a dedicated scenario with the pronounced and well documented impact of light impurities like He, C and N was implemented [9]. For this scenario, also a case was established closely matching the initial density and temperature pedestal conditions for a DIII-D reference experiment showing a pronounced impact of Li granules dropped onto the plasma [shown in figure 3 of ref. 3]. In all cases, successful Li pellet launch resulted in deep penetration and properly high but transient Li concentrations. Li sustainment times in the plasma decreased with increasing heating power from 150 to 40 ms, with the values found very similar to observed energy confinement times.

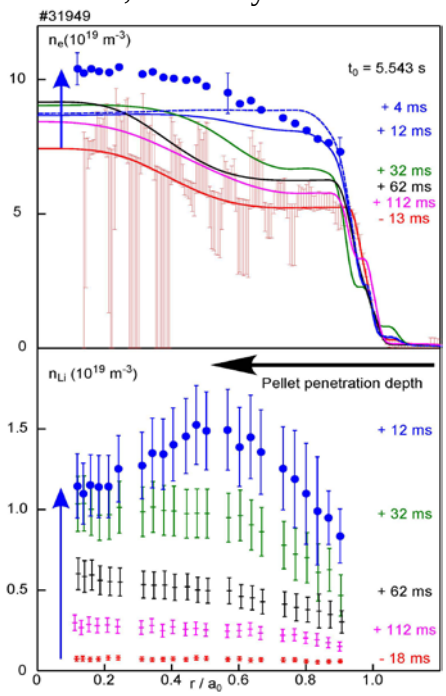

Figure 2: Temporal evolution of electron (upper) and Li density profiles after pellet injection.

EFFECT OF LI ON THE PLASMA PERFORMANCE

Investigations during system commissioning and in piggy back including the DIII-D matching were applying heating powers P_h from 3 to 12 MW, and in a dedicated plasma scenario with a proven positive sensitivity to nitrogen at P_h = 15 MW. An example of such a discharge with a sole Li pellet arriving both in a phase with and without N seeding is shown in figure 3.

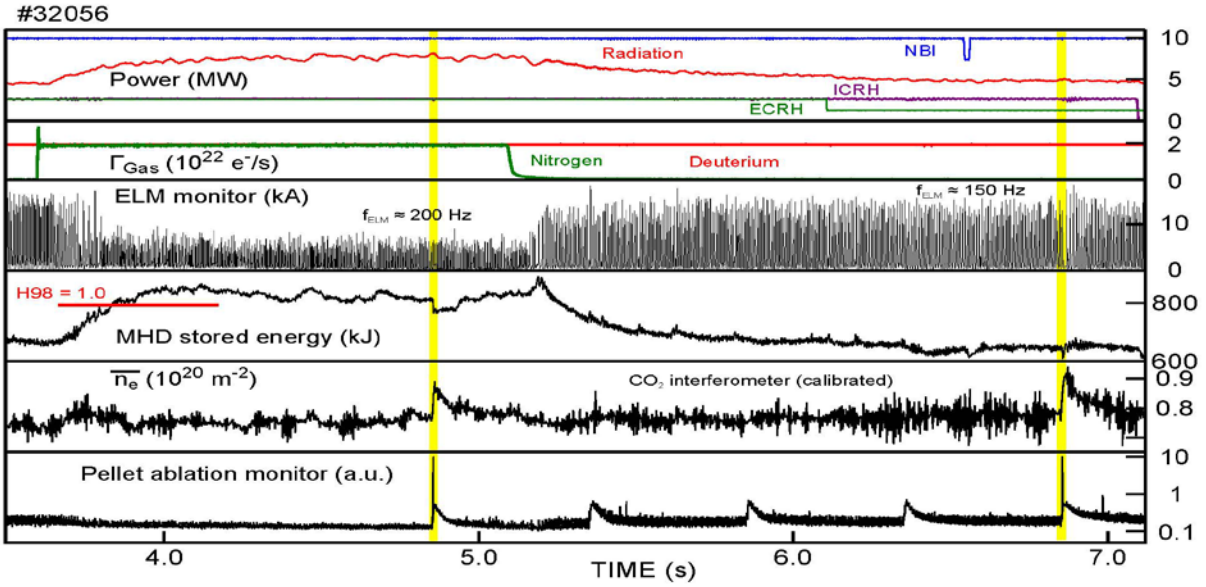

Figure 3: Dedicated discharge with N seeded and unseeded phase, arriving Li pellets indicated by yellow shaded bars. The remaining propellant gas puff adds only about 3% to the D bleeding rate.

The stored energy in the plasma turned out to be the most suitable monitor for the Li impact on the plasma performance. Injection of a Li pellet always resulted only in a small transient

change of the plasma energy. No indication of a major impact on energy or particle confinement was observed. And except for a single event, the plasma energy was only modestly reduced. For D plasmas, the magnitude of this loss decreased with increasing plasma energy until it almost vanished for the discharges with the highest heating power. We attribute this behaviour to higher Li induced radiation losses in lower energy plasmas, which is at least partially caused by their longer Li confinement time. Taking into account enhanced radiation losses and the energy consumption required for Li ablation and ionization, the dedicated high power D discharges showed indication for small (2 %) increase of the confinement. In the N seeded discharges, a significant loss of the N induced confinement surplus always took place after pellet arrival. Its magnitude cannot be explained by radiation and pellet specific losses. We attribute this to the same effect observed when applying D pellets in plasma fuelling experiments combined with N seeding. Here, the pellet driven density increase causes a loss of the achieved confinement gain.

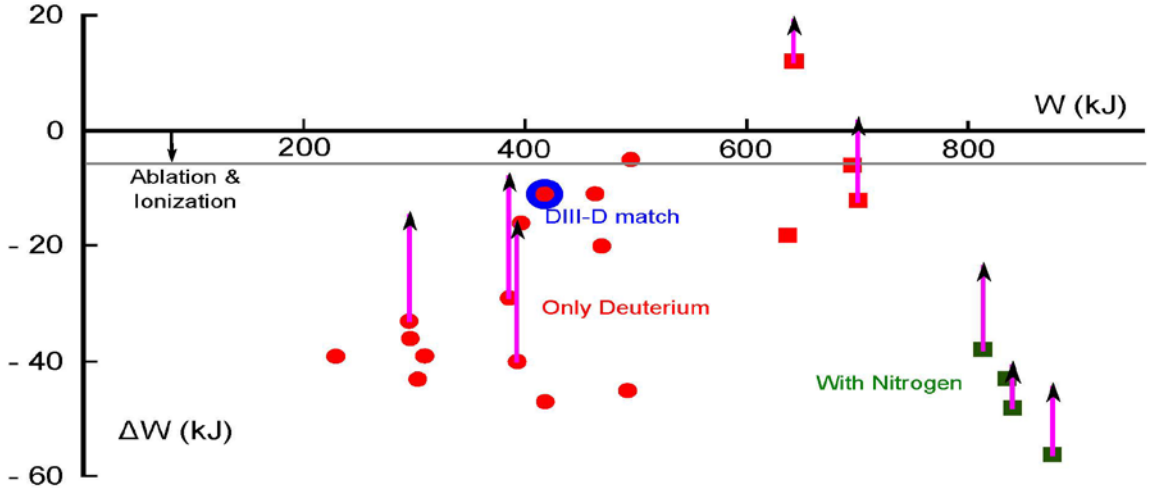

Figure 4: Pellet induced changes of the plasma energy versus initial plasma energy content. Dots: commissioning and piggy back experiments, DIII-D pedestal match indicated. Squares: dedicated experiments. Red: pure D plasmas, green: N seeding applied. Grey line: energy consumption for ablation and ionisation. Purple arrows: radiative losses caused by Li pellet.

WALL CONDITIONING EFFECTS AND ELM TRIGGER POTENTIAL

After pellet injection, a Li layer was deposited on plasma facing components, usually remaining there only for a few discharges afterwards. This short-lived wall conditioning showed modest beneficial effects during plasma start-up. Nuclear reaction analysis of tiles exposed with the divertor manipulator and extracted after the Li injection sequence revealed only very minor deposition ($< 2 \times 10^{16}$ cm^{-2}). However, at the highest heating power levels, persistent modification of surface emissivity hampered the thermography diagnostics. Li pellets showed the potential to trigger type-I ELMs, but not as reliably as required for a pacing application, e.g. as observed on EAST [4] and DIII-D [10]. Li pellet triggered ELMs show an onset time significantly longer than ELMs triggered by D pellets.

REFERENCES:

[1] H.W. Kugel et al., Phys. Plasmas **15** (2008), 056118
[2] J.S. Hu et al., Phys. Rev. Lett. **114** (2014), 055001
[3] T.H. Osborne et al., Nucl. Fusion **55** (2015), 063018
[4] D.K. Mansfield, Nucl. Fusion **53** (2013), 113023
[5] U. Stroth et al., Nucl. Fusion **53** (2013), 104003
[6] A. Herrmann et al., Nucl. Fusion **55** (2015), 063015
[7] R. Arredondo Parra et al., Rev. Sci. Instr. **87** (2016), 023508
[8] I. Erofeev et al., P1.037, this conference
[9] M. Beurskens et al., Nucl. Fusion **56** (2016), 056014
[10] A. Bortolon et al., Nucl. Fusion **56** (2016), 056008